

Review

Nanoscale Carbon-Polymer Dots for Theranostics and Biomedical Exploration

Shazid Md. Sharker ^{1,*}  and Minjae Do ²

¹ Department of Pharmaceutical Sciences, North South University, Dhaka 1229, Bangladesh

² Department of Biomedical Engineering, Johns Hopkins University, Baltimore, MD 21205, USA; mdo16@jh.edu

* Correspondence: shazid.sharker@northsouth.edu; Tel.: +880-2-5566-8200 (ext. 6402)

Abstract: In recent years, new carbonized nanomaterials have emerged in imaging, sensing, and various biomedical applications. Published literature shows that carbon dots (CDs) have been explored more extensively than any other nanomaterials. However, its polymeric version, carbon polymer dots (CPDs), did not get much attention. The non-conjugated and single-particle CPDs have all the merits of polymer and CDs, such as photoluminescent properties. The partially carbonized CPDs can be applied like CDs without surface passivation and functionalization. This merit can be further enhanced through the selection of desired precursors and control of carbonization synthesis. CPDs can absorb UV-visible-NIR light and can enhance the photoresponsive chemical and biochemical interactions. This review aims to introduce this area of renewed interest and provide insights into current developments of CPDs nanoparticles and present an overview of chemical, biological, and therapeutic applications.

Keywords: carbon polymer dots (CPDs); nanoscale correlations; photo-response; biochemical applications; therapeutic applications



Citation: Sharker, S.M.; Do, M. Nanoscale Carbon-Polymer Dots for Theranostics and Biomedical Exploration. *J. Nanotheranostics* **2021**, *2*, 118–130. <https://doi.org/10.3390/jnt2030008>

Academic Editor: Dong-Wook Han

Received: 9 June 2021

Accepted: 27 July 2021

Published: 29 July 2021

Publisher's Note: MDPI stays neutral with regard to jurisdictional claims in published maps and institutional affiliations.



Copyright: © 2021 by the authors. Licensee MDPI, Basel, Switzerland. This article is an open access article distributed under the terms and conditions of the Creative Commons Attribution (CC BY) license (<https://creativecommons.org/licenses/by/4.0/>).

1. Introduction

Carbon polymer dots (CPDs) are a member of carbon dots (CDs) and possess a hybrid structure of carbon core attached with organic polymer chains. CPDs are synthesized from different polymer precursors and small organic molecules using controlled carbonizations, dehydration, hydrothermal, and condensation (Figure 1). The controlled carbonizations allow the generation of large functional groups on its surface and play a significant role in maintaining hybrid properties between polymer and CDs. The abundant energy levels in CPDs increase the probability of intersystem crossing (ISC), and their covalently cross-linked framework structures significantly suppress the nonradiative transitions. Moreover, the “core-shell” structures of CPDs are identical compare with a carbon-based and small molecular fluorophore. The center core contributed emission center that retains outer polymer shell [1,2].

The photoluminescent (PL) properties of CPDs are distinguished from organic fluorophores by nonconjugated sub-fluorophores, including C=N, C=O, N=O, C-O, and different hetero-atom containing double (=) bonds. Fortunately, these sub-fluorophores' fluorescence in PCDs can be enhanced through physical immobilization or chemical cross-linking of polymer chains, which is entitled to the enhanced cross-link emission (CEE) effect. The low synthesis cost, unique structures, low toxicity, and excitation-dependent luminescence are among a few of the growing attractive merits of CPDs [3,4].

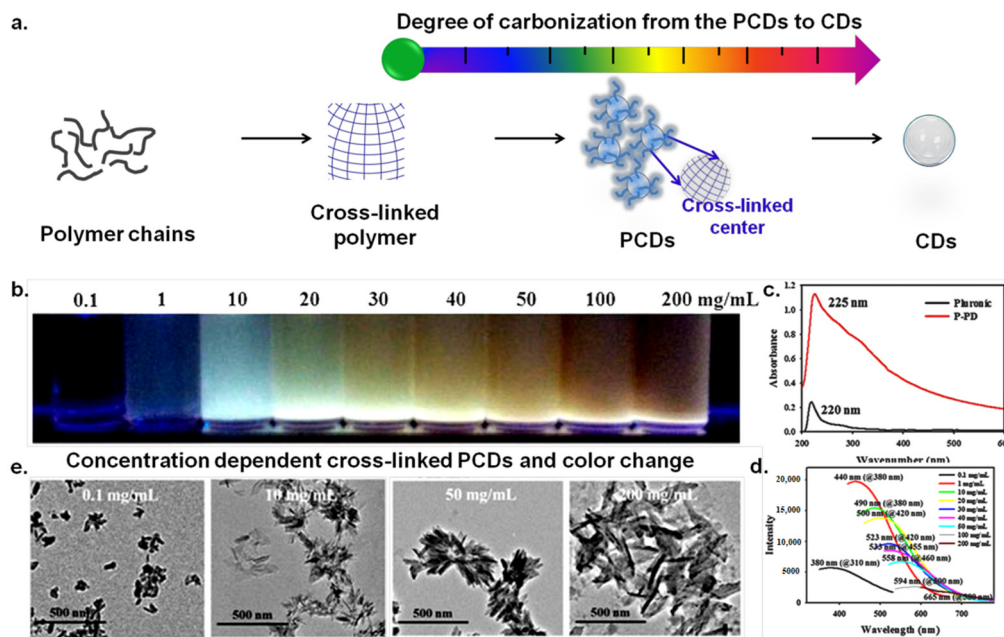


Figure 1. (a) The schematic diagram illustrates the cross-linking and degree of carbonization of the carbon polymer dots (CPDs) and carbon dots (CDs). (b) The photoluminescence (PL) behaviors of polymer carbon dots (PCDs)-based on cross-linking and concentration. (c) The absorption spectrum of precursor PCDs and after synthesis of PCDs (P-PD). (d) The concentration dependent fluorescence emission spectrum of PCDs. (e) The TEM images of CPDs indicates the polymeric properties and cross-linked nature. Reprinted with permission from ref. [5] Copyright© 2015 John Wiley & Sons, Ltd.

2. Carbon Polymer Dot (CPDs), Carbon Dots (CDs) and Polymer Dots (PDs)

The most familiar CDs are low-dimensional carbon-based nanoparticles (NPs). The NPs are typically ~20 nm size and sp²/sp³ hybrid carbon composition. The carbonization reaction in the hydrated media, as well as the precursor source of CDs, contributed to a large number of functional groups on its surface including, amine (-NH₂), hydroxyl (-OH), and carboxylic (-COOH) groups. The CDs' surface functional groups can be a conjugated ligand to link other organic and inorganic materials. However, in its polymeric version, the carbon polymer dots (CPDs) belong to a center core carbon with a nonconjugated hybrid polymeric structure. The dominant polymeric parts in CPDs mainly determine the faith of this nanoscale material. Therefore compare to CDs, its hybrid form of CPDs shows better optical and photoluminescence quantum yield (PLQY) [1].

CPDs hold three unique properties. First, the incomplete carbonization results in a low molecular weight chain and many functional groups. Second, the reaction condition in the complex polymerization generates polydispersity on the PCDs structure. Lastly, dehydration and carbonization are attributed to the distinctly cross-linked network structure. On the other hand, the typical polymer dots (PDs) have a shortage of this identical cross-link feature. All of these properties are different compared with un-carbonized PDs and completely carbonized CDs [1,6,7].

In general, the partial carbonizations of polymer precursor sources have generated CPDs (Table 1). Therefore, the level of carbonization determines the functional and structural identity of hybrid PCDs polymer-carbon nanoparticles. The CDs' post-decoration can also reach the CPDs with polymer or organic molecules. The CPDs prepared by post-decoration have possessed the complete core structures of CDs with a clear boundary between the core and polymer shell. The carbon core of CPDs is supported to be the full carbonization core, concretely similar to CDs' core structures. The cores can show intrinsic state or sub-domain state emission, respectively, or a semi-crystalline carbon core structure composed of tiny carbon clusters surrounded by polymer frames or a partly dehydrated

cross-linking close-knit polymer structure core that can be an ordered carbon skeleton structure [1,8].

The nanoscale carbon core appears like a sub-domain in CPDs, which are considered pi-conjugated graphene (G) and diamond (D) like hybrid structures. The pi-conjugated could also appear like a fullerene structure. As a result, studies show amorphous structural properties of CPDs. In one notable report, the CPDs demonstrated a needle-like shape on the TEM (transmission electron microscopy) [5]. Other reports also show 0.20 nm lattice spacing of CPDs on the high-resolution transmission electron microscopy (HR-TEM). The studies also demonstrated a thin amorphous layer on every side of CPDs. At the same time, the X-ray diffraction patterns showed identical peaks around 18.7° and interlayer spacing of 0.47 and 0.34 nm, respectively. This could be due to the hybridized structural effects of polymer and carbonized parts. Therefore, sustained optical absorption and long-term aqueous stability of CPDs was demonstrated well suited for biomedical exploration [2,5].

The large surface functional groups and sustain photostability are one of the iconic merits of CPDs. The FT-IR and XPS report in different studies has shown many carbon, nitrogen, and oxygen-containing functional groups. As most of the CPDs synthesize by surface oxidation during pyrolysis, oxygen-containing functional groups dominate. In other literature, it has also been found that CPDs can provide rapid optical response potential for biomedical sciences [5].

The transmission electron microscope (TEM) images usually determine the size of any nanoparticles like carbon-polymer dots and non-carbon dots. The size distribution can be measured using dynamic light scattering (DLS) and surface charge through a zeta sizer. All of these data were used to recognize nanoparticles' size and shape. The differences between CPDs and CDs can be compared in TEM and DLS analysis. In the case of CPDs, the size determined in DLS measurements was bigger than TEM (size) results. The result (larger size) explained the extension of polymeric parts presence on the CPDs in the aqueous-based DLS study. However, such prominent size differences were not noticed in CDs analysis due to lack of polymer moiety [6].

In some cases, the scanning electron microscope (SEM) with energy-dispersive X-ray spectroscopy (EDX) are combined (SEM/EDX) and used to determine the size and elemental composition measurements. Additionally, X-ray photoelectron spectroscopy (XPS), nuclear magnetic resonance (NMR) spectroscopy, and infrared (IR) have provided valuable information about the nature of the composition, either it is carbon-polymer dots or carbon dots. In the XPS analysis, the higher percentages of sp² type carbon at 284 eV and a π - π^* transition peak appeared at 292 eV for the CDs were different identities compare with CPDs. At the ¹H-NMR signal, the respective peaks of the precursor (polymer) sources were found to be a presence in the CPDs nanocomposite, but no meaningful (polymeric) peaks were observed in the CDs materials [9,10]. As both are carbon-based nanomaterials, the Raman spectroscopic D and G band can identify the ratio of carbon-carbon single and carbon=carbon double bond [9–11].

The incomplete or partial carbonizations of CPDs have molded polymeric merit with many surface functional groups. The chemical functional groups can work as a reactive bridge to, linked with others that are advantageous for requiring modification. Furthermore, the low toxicity and biocompatibility, and simple process-ability are more promising for biological application than organic dyes or inorganic quantum dots (QDs) [11].

The carbon skeleton and surface polymeric functional groups of CPDs have been made identical from a single molecular state. The identical hybrid structures provided synergistic effects for photoluminescence (PL). Many reports believe that sub-fluorophores where extended pi-electron and surface chemistry work together to create an energy gap of the surface state. The new sub-levels on the pi-electronic system with electrons and holes (e/h) pair recombine, which play an essential role in photoluminescence (PL) [3]. The sub-levels on PCDs can be created during synthesis through surface oxidation or others methods.

3. Current Status and Correlation of Different CPDs

At present, the hydrothermal route has been used to synthesize CPDs from various sources (Table 1).

Table 1. The representative examples of Carbon Polymer Dots (CPDs) and their synthesis conditions including, reaction time, temperature, solvent and reaction yield.

| No. | Precursors (Sources) | Synthesis | Reaction Time | Temperature and Solvent | Yield | Ref. |
|-----|---|---|---------------|--|----------------|------|
| 1 | Polyacrylic acid and ethylenediamine | Hydrothermal | 8 h | 200 °C, deionized water | 30% | [12] |
| 2 | Polyacrylic acid (PAA) and ethylenediamine (EDA) | Hydrothermal | 8 h | 200 °C, deionized water | 63.10% | [10] |
| 3 | Chitosan | Hydrothermal | 3 h | 180 °C, deionized water | - | [13] |
| 4 | Citric acid and ethylenediamine | Hydrothermal | 5 h | 160 °C, distilled water | - | [14] |
| 5 | Tris(2-aminoethyl)amine and citric acid | Hydrothermal | 6 h | Appropriate temperature, water | - | [15] |
| 6 | Polyvinyl alcohol | Hydrothermal | 6 h | 220 °C, deionized water | - | [16] |
| 7 | Disulfide-crosslinked hyaluronic acid | Hydrothermal | 8 h | 180 °C, deionized water | - | [17] |
| 8 | L-serine and L-tryptophan | Hydrothermal | 8 h | 300 °C, alkaline water (about pH 4) | - | [18] |
| 9 | Acrylamide and N,N'-Methylenebisacrylamide | Hydrothermal addition polymerization and carbonization strategy | 8 h | 200 °C, deionized water | - | [19] |
| 10 | Acrylamide and N,N'-Methylenebisacrylamide | Hydrothermal condensation crosslinking and carbonization | 8 h | 200 °C deionized water | 86.7% to 84.6% | [20] |
| 11 | Citric acid and ethylenediamine | Low Heating | 3 min | 140 °C, ultrapure water | 35% | [21] |
| 12 | Polypropylene (PP) plastic waste | Heating at 200–300 °C | 20 min | 200–300 °C, ethanol | - | [22] |
| 13 | Polymerization of ascorbic acid and polyethylenimine | Dehydration by phosphoric acid | 5 h | 90 °C, 5M phosphoric acid | - | [23] |
| 14 | Pluronic® F-127 | Dehydration by Sulfuric acid | 1 min | 100 °C, H ₂ SO ₄ | 17% | [24] |
| 15 | Polyethyleneimine and carbon tetrachloride | Dehydration | 5–6 h | 90–200 °C, deionized water | - | [25] |
| 16 | Phenylenediamine | Dehydration by HNO ₃ | 10 h | 200 °C, H ₂ SO ₄ | - | [26] |
| 17 | o-phenylenediamine, mphenylenediamine, p-phenylenediamine | Oxidative polymerization using HNO ₃ and H ₂ O ₂ | 12 h | Room temperature, HNO ₃ | - | [27] |
| 18 | 1,8-naphthalenediol | Using n-propanol solvents | 8 h | 150 °C, n-propanol | - | [28] |
| 19 | p-phenylenediamine | Oxidative polymerization at 80 °C | 36 h | 80 °C, water | - | [29] |
| 20 | Polyvinyl alcohol and Ethylene diamine | Microwave-assisted method | 1.50 h | 200 °C, water | - | [30] |
| 21 | Maleic acid and ethylenediamine | Microwave-assisted | 20 min | 1000 W, deionized water | 89% | [30] |
| 22 | Polyethyleneimine | Pyrolytic method | 30 min | 180 °C, ultrapure water | - | [31] |
| 23 | Branched polyethylenimine | Controlled decomposition | 10 min | 200 °C, ethanol | - | [32] |
| 24 | Citric acid (CA) and urea | Heat-treatment | - | 85 °C, water | 3.75% | [33] |
| 25 | p-phenylenediamine and FeCl ₃ | Heat-treatment | 24 h | 120 °C, ultrapure water | - | [34] |
| 26 | Taxus leaves deep | Solvo-thermal procedure | 5 h | 120 °C, acetone | 1% | [35] |

Table 1. Cont.

| No. | Precursors (Sources) | Synthesis | Reaction Time | Temperature and Solvent | Yield | Ref. |
|-----|---|-------------------------|---------------|-------------------------|-------|------|
| 27 | Ethylenediamine and carbon tetrachloride | Polymerization reaction | 6 h | 90 °C, deionized water | - | [36] |
| 28 | Hyperbranched polyethyleneimine and 5-aminosalicylic acid | Amidation reaction | 12 h | 80 °C, water | - | [37] |
| 29 | Ascorbic acid and diethylenetriamine | - | 72 h | 200 °C, water | - | [38] |
| 31 | p-Phenylenediamine | - | 24 h | 80 °C, water | - | [39] |

The exothermic reaction of hydrothermal carbonization facilitated the conversion of organic compounds to structured carbons [8,10–16]. Both low temperature and high temperature were used in this regard for desired carbonization [19]. The reaction can be stopped in several stages for incomplete elimination of water or carbonization that results from the synthesis of partial carbonized CPDs. Several other studies show the controlled dehydration against carbon sources using the strong acid-assisted synthesis of CPDs [22–24]. The solvothermal, microwave heat-based and regulated chemical reactions were used to achieve desired carbonization and synthesis of CPDs [28,33]. At the end of synthesis, centrifugation, dialysis, or electrophoresis were used to separate and purify CPDs. At the same time, the chromatography can be used for the purification of CPDs.

In general, a hydrothermal process, a dehydration reaction, or a microwave-assisted method can be used to synthesize CDs and CPDs. In the case of CPDs synthesis, the reaction condition needs to optimize for the required CPDs. For example, the chemical and fluorescence properties need to evaluate at a different time (5 min, 10 min, 20 min, or 30 min) of dehydration reaction. The exact reaction time that allows required CPDs depends on the nature of the polymer precursor source and the dehydration reaction environment. However, the maximum dehydration at a specific reaction time resulting vanish all polymeric precursors, which results in the CDs [1,3,7]. For example, 1.5 min dehydration of Hyaluronic Acid (HA) by H₂SO₄ (30N) shown partial carbonized CPDs (Hyaluronic Acid Fluorescent Carbon Nanoparticle) and 10 min dehydration generated CDs (Fluorescent Carbon Nanoparticle). The carbonization of fewer than 1.5 min did not show any noticeable fluorescence, and carbonizations of fewer than 10 min were allowed CPDs formation. The critical point was that the reaction conditions needed to be finely adjusted to get a higher yield and controlled the carbonization reaction [39].

The specific nanoparticles with polymeric hybrid structures have allowed explorations of different promising applications. Both unmodified and modified CPDs including doped CPDs are potential for metal ions sensing. The inherent PL properties showed fluorescence-based detection of different metal ions including, Cr (VI), Co²⁺, and Mn²⁺ (Table 2) [28,33,40]. Furthermore, the room-temperature phosphorescence, light-emitting diodes and photocatalysis applications against CPDs are very promising [8,17,31]. Different notable studies demonstrated that polymer-based CPDs could be used as skin sensors to monitor pathophysiological conditions, including cancer [15,25]. In the anti-counterfeit materials, pH probe and photocatalytic exploration of CPDs are among the few areas that get considerable attention [13,14,18]. Moreover, the biocompatibility of CPDs is demonstrated through the hepatobiliary system and kidney eliminations that can work towards in biomedical sciences including, the drug delivery system [33]. Therefore the notable studied confirmed that CPDs are promising for drug (doxorubicin)-loading, Photodynamic Therapy (PDT), and theranostics applications [11,23,24,32].

Table 2. The representative examples of CPDs and their fluorescence quantum yield (QY), excitation and emission wavelength and applications.

| No. | Precursors (Sources) | Fluorescence Quantum Yield | Excitation and Emission Wavelength | Application | Ref. |
|-----|---|----------------------------|---|---|------|
| 1 | Polyacrylic acid and ethylenediamine | 44.18% | 340 nm and 410 nm | Fluorescence detection | [12] |
| 2 | Polyacrylic acid (PAA) and ethylenediamine (EDA) | 2.13–32.41% | 410 nm and 494 nm | Metal-free Room-temperature phosphorescence (RTP) materials | [10] |
| 3 | Chitosan | 66.81% | Excitation dependent emission | Doxorubicin-loading | [13] |
| 4 | Citric acid and ethylenediamine | - | - | Cr (VI) detects in domestic water | [14] |
| 5 | Tris(2-aminoethyl)amine and citric acid | 64.5% | 240–360 nm and 445 nm | pH and excellent fluorescent properties | [15] |
| 6 | Polyvinyl alcohol | - | 365 nm and 402–470 nm | With TiO ₂ demonstrate excellent photocatalytic activity | [16] |
| 7 | Disulfide-crosslinked hyaluronic acid | - | - | Skin sensor and sensitive cancer detection | [17] |
| 8 | L-serine and L-tryptophan | 89.57% | 300 to 420 nm and 489 to 505 nm | Room-temperature ferromagnetism (RTFM) | [18] |
| 9 | Acrylamide and N,N'-Methylenebiacrylamide | 89% | 320 nm and 380 nm | Room-temperature phosphorescence (RTP) properties | [19] |
| 10 | Acrylamide and N,N'-Methylenebiacrylamide | 45.58% | excitation-independent and 320 nm to 380 nm | Anti-counterfeit applications | [20] |
| 11 | Citric acid and ethylenediamine | 13–64% | 350–390 nm and 445–470 nm | Metal ion sensing | [21] |
| 12 | Polypropylene (PP) plastic waste | - | 400–435 nm and 410–440 nm | Environmental conservation | [22] |
| 13 | Polymerization of ascorbic acid and polyethylenimine | 3.8% | 350 nm and 487 nm | NO ₂ ⁻ analysis in water and milk, and monitoring of nitrite entry into Hep-2 cells | [23] |
| 14 | Pluronic® F-127 | 3.32% | 365 nm and 470 nm | Multi-color fluorescence | [24] |
| 15 | Polyethylenimine and carbon tetrachloride | 2.7% | 400 nm and 475 nm | Cellular uptake mechanism and internalization | [25] |
| 16 | Phenylenediamine | 10.83–31.54% | 540 nm and 630 nm | Theranostics and real-time diseases tracking | [26] |
| 17 | o-phenylenediamine, mphenylenediamine, p-phenylenediamine | - | 370–470 nm and 463–550 nm | Detect breast cancer & cancer diagnosis | [27] |
| 18 | 1,8-naphthalenediol | 2–14.8% | 440 nm and 570–610 nm | Water detection in organic solvents | [28] |
| 19 | p-phenylenediamine | 7% | 200–350 nm and 350–750 nm | Monitoring the pH fluctuation in HeLa cells | [29] |
| 20 | Polyvinyl alcohol and Ethylene diamine | 54% | 290–380 nm and 340–390 nm | Cobalt ion (Co ²⁺) and manganese ion (Mn ²⁺) detection | [30] |
| 21 | Maleic acid and ethylenediamine | 8.50% | 365 nm and 460–625 nm | Self-quenching-resistant solid-state fluorescent | [30] |
| 22 | Polyethylenimine | 9% | 365 nm and 320–460 nm | Metronidazole detection in Milk samples | [31] |
| 23 | Branched polyethylenimine | 13.3% to 58% | 365 nm and 465 nm | Fluorescent paint, and to deposit durable coatings on glass substrates | [32] |
| 24 | Citric acid (CA) and urea | 11.2% | 330–389 nm and 380–750 nm | White light-emitting diodes (WLEDs) | [33] |
| 25 | p-phenylenediamine and FeCl ₃ | - | 300–400 nm and 400–550 nm | Photodynamic therapy (PDT) for the treatment of cancer | [34] |
| 26 | Taxus leaves deep | 31–59% | 350–680 nm and 413–750 nm | Biocompatible through excreted via kidneys and hepatobiliary system | [35] |
| 27 | Ethylenediamine and carbon tetrachloride | 8.6–17.3% | 340–460 nm and 440–520 nm | Adsorption capabilities for transition-metal ions | [36] |

Table 2. Cont.

| No. | Precursors (Sources) | Fluorescence Quantum Yield | Excitation and Emission Wavelength | Application | Ref. |
|-----|---|----------------------------|------------------------------------|--|------|
| 28 | Hyperbranched polyethyleneimine and 5-aminosalicylic acid | 53.3% | 350–400 nm and 482–506 nm | Environmental monitoring | [37] |
| 29 | Ascorbic acid and diethylenetriamine | 47% | 350 nm and 430 nm | Intracellular imaging of ferric ions in HeLa cells | [38] |
| 30 | p-Phenylenediamine | 2.35–4.95% | 330–400 nm and 460–600 nm | Optical responses to H ₂ O and D ₂ O | [39] |

4. Bio-Conjugation and Surface Functionalization

CPDs have shown different types of chemical functional groups, including COOH and -OH that can integrate with other materials. For example, CPDs that conjugate therapeutic agents could perform medical imaging and anticancer activity and real-time tracing for diagnosis and therapeutic monitoring. The combined diagnosis and therapeutic, commonly known as theranostic, can be a promising area for CPDs. Additionally, the CPDs integrated nanomaterials can be a potential candidate for thermo- and pH-responsive drug delivery, photo-optical temperature sensing, photothermal and photodynamic therapy, and other biomedical sciences [41]. Therefore, we can expect that many exciting explorations are waiting in the study of the polymeric characteristic of CPDs.

The distinguishing property of CPDs is randomness in polymeric type structure and polydispersity. Due to the mixed presence of polymer chains and carbon clusters during synthesis, it is most analogous to typical polymeric property. The reaction synthesis condition including temperature, time, and pH, determines the nature of CPDs. As a result, variability in structure has been found in its structures. Therefore optical properties are also affected owing to differences in size and morphology [4]. It is imperative in the case of improved quasi-mono-dispersed CPDs.

CPDs have shown a strong absorption band near the UV area and a broad spectrum from visible to NIR region. The hybrid carbon-polymeric structures and polydispersity are mainly responsible for the broad absorption spectrum. In CPDs, the carbonized parts mainly exhibited π - π^* type transition while the surface functional groups and lone pair electron contributed n - π^* transition. The size-related quantum confinement effects and energy bandgap can be a liable factor of identical light absorption bands. Moreover, the dense carbon parts in the CPDs and different groups could be a reason for generating the energy gap. The size variation due to polydispersity and surface chemistry might combinedly control the characteristic of optical property. As the mechanism of optical absorption of CPDs is still unclear, more studies are required to make satisfactory elusive [4].

The difficulties in determining the mechanism of CPDs' optical absorption properties are mainly because of the large hetero-atom. It is related to carbon-polymer hybrid configuration. Some studies proposed the similarity relation between fluorescent polymer materials and CPDs optical behavior. The fluorescent polymeric materials belong to fluorescent molecules conjugated polymer. The heteroatom like C-O, C-N, and N-O on the fluorescent polymeric materials works like a fluorophore. In this configuration, the polymeric chain works to decrease the energy bandgap resulting emission of fluorescence energy [4,42].

5. Biomedical and Theranostic Applications of Carbon Polymer Dots (CPDs)

The advancement in low-dimensions nanomaterials drug-carrier has rapidly translated into clinical practice. Interestingly, the one-dimensional (1D) nanomaterials of carbon dots (CDs) are relatively well-explored compared with their polymeric version, carbon polymer dots (CPDs). However, the unique polymeric properties of CPDs nanomaterials make them well-suited for the different biomedical fields. Recent studies have shown that CPDs are potential candidates in biomedical sciences, both as nanocarriers and nanotransducers [43–46]. CPDs are a potential candidate for the researcher to develop novel functional materials. The conjunctions of required organic and inorganic building moieties

into the CPDs have made it more realistic [1]. Furthermore, the unique fabrication of CPDs with other bioactive molecules has been demonstrated in different published reports. Therefore, it is expected that CPDs can be more attractive than carbon dots (CDs) [7,24]. For example, CPDs like CDs could deliver the anticancer drug to its targeted area and perform the theranostic activity (Figure 2).

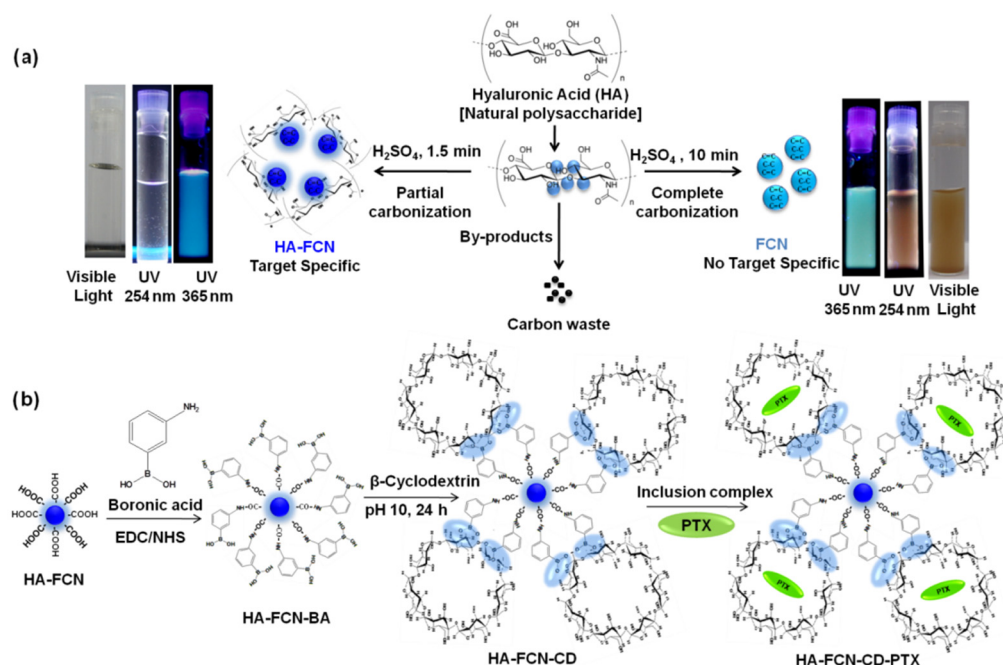


Figure 2. (a) Scheme of partial carbonized hyaluronic acid-fluorescent carbon nanoparticle (HA-FCN) and complete carbonized FCN (fluorescent carbon nanoparticle) preparation from hyaluronic acid (HA). An illuminated photograph of aqueous solutions of HA-FCN and FCN under visible light, and 254 nm and 365 nm UV lamps, respectively. Reprinted with permission from ref. [10] Copyright© 2015, The Royal Society of Chemistry. (b) The synthesis of Paclitaxel (PTX) complexed HA-FCN-CD [HA-FCN-Cyclodextrin-PTX] for tumor targeted bioimaging guided drug delivery. Reprinted with permission from ref. [47] Copyright© 2015, The Royal Society of Chemistry.

In one notable study, the controlled carbonization method using hyaluronic acid (HA) results from partial-carbonized HA-FCN with remaining HA (Figure 2). Hyaluronic acid (HA) is commonly used in tumor-targeted drug delivery owing to CD-44 receptor binding affinity. The noticeable exploration showed in vivo for targeted delivery and bio-imaging potentials. Moreover, fully carbonized the fluorescent carbon nanoparticle (FCN) from the same sources resulted in a biocompatible bioimaging probe [46]. Further extension of this notable study found HA-FCN conjugated with boronic acid to form diol-linkage with cyclodextrin. Finally, the chemotherapeutic paclitaxel was part of the inclusion complex into HA-FCN conjugated cyclodextrin. Their novel attempts have allowed for controlling drug release in response to extracellular tumor environment (pH) and external-remote photo thermally [47]. These facts have fueled efforts to develop a robust drug delivery system that can bring new hope for cancer treatment.

The most attractive properties of these CPDs for biological applications are the broad absorption of light in the UV-Vis-NIR region, photoluminescence, exceptional photo-response, photosensitized production of singlet oxygen, and vast surface area for the covalent and non-covalent anchoring of diagnostic agents and drugs/DNA/RNA. Furthermore, the functionalized CPDs showed promising results in biosensing. In one studied, α -l-Fucosidase (AFu) diseases biomarker was evaluated using hydrolyzate of 4-nitrophenyl- α -l-fucopyranoside on the functionalized CPDs [48]. Therefore, drug and gene delivery, photothermal or photodynamic therapy, biosensing, and medical imaging are promising areas for CPDs [4,49,50].

The nanoscale based nano-fabrication is a very emerging research area. The typical metal ion sensing required lengthy and complex instrumental spectroscopic techniques. However, the carbonized CPDs have stable optical properties that could be utilized in electrochemistry and wastewater treatment to absorb and separate metal ions. In one notable study, the researcher successfully measured Cu^{2+} ions using nano-fabricate CPDs. The low-cost, straightforward, and effective methods in this finding could be extended to other similar platforms (Figure 3) [51,52].

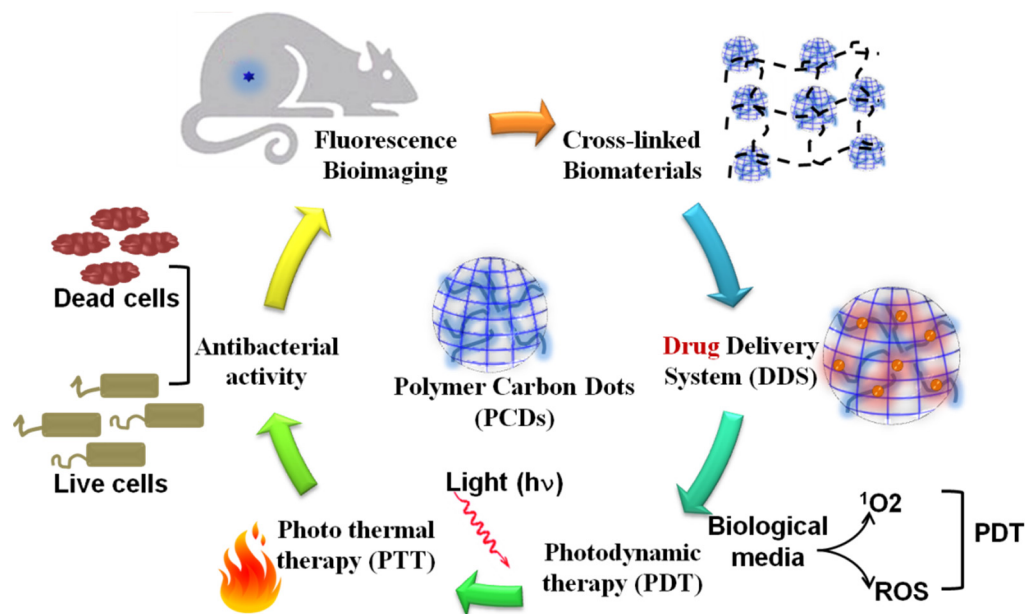


Figure 3. Schematic description of PCDs based different delivery system and their potential biomedical applications.

The remarkable optical properties of CPDs and cross-linked polymeric properties have inspired potential applications in biomedical sciences [53,54]. The cytocompatibility and bioimaging merits of CPDs demonstrated on KB (human oral squamous carcinoma) cells. The minimum cytotoxicity against CPDs was shown on the MTT assay. The empirical finding suggested that CPDs could be used in high concentrations in vivo [54,55]. The intravenous injection mouse studies against mouse was exhibited in vivo bioimaging potentiality. The emission wavelength recorded 600 nm in response to 540 nm excitation wavelength that is a potential for fluorescence bioimaging [56].

The targeting drug delivery system (DDS) is crucial for improving tumor area-specific drug release and therapeutic efficacy [57,58]. At present, different light-responsive nanomaterials have been studied as upcoming anticancer drug carriers. In this platform, the successful targeting with light-responsive nanomaterials could be used as PDT by generating toxic reactive oxygen species (ROS). It could also be used as PTT by producing heat to kill the cancer cells thermally (Figure 3) [32]. The polymer with carbonized CDs in response to excitation light can utilize area-specific cancer therapy. The photo-responsive CPDs could use like CDs for the development of essential therapeutic materials [59,60].

At the same time, photothermal-dependent light-responsive CPDs could be employed in temperature-controlled drug delivery and photothermal chemotherapy [61,62]. In this arena, the inorganic metal oxide nanoparticles and fully carbonized graphene oxide, CDs, and carbon nanotubes are well-recognized materials; however, CPDs did get much recognition in the research community [63–68]. For instance, the polymeric nature of CPDs can load maximum drug on its lengthy chain to perform a light-triggered controlled drug release upon irradiation.

Photo-responsive CPDs are also potentially light harvesting; with potential for photocatalysis application [69]. Studies showed presences of abundant functional groups can

regulate electron-donating or withdrawing function. Therefore, the $-NH_2$ or $-COOH$ functional groups containing CPDs act as cathode or anode interlayers for the development of polymer solar cells (PSCs) [70].

6. Perspective and Future Directions

Carbon polymer dots (CPDs) are a new variant of well-known carbon dots (CDs). The distinctive polymer/carbon hybrid structure, low degree of carbonization, nonconjugated fluorescent polymeric nature, and high degree of crosslinking have made CPDs the most promising candidate in other biomedical explorations. CPDs gained tremendous attention in the biology field because of high water solubility, high quantum yield, low toxicity, surface functionalization, and accessible synthesis methods. The synthesis methods of CPDs with changing morphology are still unclear due to the lack of systematic structure characteristics and complex polymer/carbon hybrid features. However, the controlled synthesis of desired CPDs can contribute to bioimaging, biosensing, biomedicine, and drug delivery systems. The hybrid polymeric nature of CPDs provided easy surface functionalization according to desired properties like blending, grafting, and covalent bonding with the functional molecule, polymer, or inorganic materials. It will explore the enormous possibility of targeted drug delivery, phototherapy, medical bioimaging, and small molecule and ion detection. The previous researches of photoresponsive CPDs are very promising because of small sizes, functionalization potentiality, and the ability to introduce multiple therapeutic agents on its surface. A collective effort from nanotechnology has required the development of cancer theranostic to overcome the hurdle of translating photoresponsive CPDs.

7. Conclusions

The cooperative effort from nanotechnology needs to synthesize carbon polymer dots (CPDs) for biomedical application. Though scale-up synthesis and purification of CPDs are still challenging, the photophysical and biocompatible properties are up-and-coming. Moreover, different bioactive therapeutic can be anchored to its surface to develop a brand-new drug delivery system (DDS). The combined therapeutic with diagnostic nanoparticles (NPs) known as theranostics NPs, set a potential site for CPDs. The exploration of CPDs is still in the early stage; however, the preliminary works are so attractive to shift the paradigm of traditional NPs. Therefore, the unique properties of CPDs are expected to translate their potential role clinically.

Author Contributions: Conceptualization, S.M.S.; writing—review and editing, S.M.S. and M.D. All authors have read and agreed to the published version of the manuscript.

Funding: This research received no external funding.

Acknowledgments: The corresponding author is thankful to the CTRGC-NSU (CTRG-2020-2021/SHLS/No.1001) authority to support study and research in the Department of Pharmaceutical Sciences, North South University, Dhaka, Bangladesh.

Conflicts of Interest: The authors declare no conflict of interest.

References

1. Xia, C.; Zhu, S.; Feng, T.; Yang, M.; Yang, B. Evolution and Synthesis of Carbon Dots: From Carbon Dots to Carbonized Polymer Dots. *Adv. Sci.* **2019**, *6*, 1901316. [[CrossRef](#)]
2. Song, Y.; Zhu, S.; Shao, J.; Yang, B. Polymer carbon dots—A highlight reviewing their unique structure, bright emission and probable photoluminescence mechanism. *J. Polym. Sci. Part A Polym. Chem.* **2017**, *55*, 610–615. [[CrossRef](#)]
3. Shao, J.; Zhu, S.; Liu, H.; Song, Y.; Tao, S.; Yang, B. Full-Color Emission Polymer Carbon Dots with Quench-Resistant Solid-State Fluorescence. *Adv. Sci.* **2017**, *4*, 1700395. [[CrossRef](#)] [[PubMed](#)]
4. Tao, S.; Zhu, S.; Feng, T.; Xia, C.; Song, Y.; Yang, B. The polymeric characteristics and photoluminescence mechanism in polymer carbon dots: A review. *Mater. Today Chem.* **2017**, *6*, 13–25. [[CrossRef](#)]
5. Jeong, C.J.; Lee, G.; In, I.; Park, S.Y. Concentration-mediated multicolor fluorescence polymer carbon dots. *Lumin* **2015**, *31*, 897–904. [[CrossRef](#)] [[PubMed](#)]

6. Gu, J.; Wang, W.; Zhang, Q.; Meng, Z.; Jia, X.; Xi, K. Synthesis of fluorescent carbon nanoparticles from polyacrylamide for fast cellular endocytosis. *RSC Adv.* **2013**, *3*, 15589–15591. [[CrossRef](#)]
7. Song, Y.; Zhu, S.; Zhang, S.; Fu, Y.; Wang, L.; Zhao, X.; Yang, B. Investigation from chemical structure to photoluminescent mechanism: A type of carbon dots from the pyrolysis of citric acid and an amine. *J. Mater. Chem. C* **2015**, *3*, 5976–5984. [[CrossRef](#)]
8. Tao, S.; Lu, S.; Geng, Y.; Zhu, S.; Redfern, S.A.T.; Song, Y.; Feng, T.; Xu, W.; Yang, B. Design of Metal-Free Polymer Carbon Dots: A New Class of Room-Temperature Phosphorescent Materials. *Angew. Chem. Int. Ed.* **2018**, *57*, 2393–2398. [[CrossRef](#)]
9. Liu, B.; Chu, B.; Wang, Y.-L.; Hu, L.-F.; Hu, S.; Zhang, X.-H. Carbon dioxide derived carbonized polymer dots for multicolor light-emitting diodes. *Green Chem.* **2020**, *23*, 422–429. [[CrossRef](#)]
10. Sharker, S.M.; Kim, S.M.; Lee, J.E.; Jeong, J.H.; In, I.; Lee, K.D.; Lee, H.; Park, S.Y. In situ synthesis of luminescent carbon nanoparticles toward target bioimaging. *Nanoscale* **2015**, *7*, 5468–5475. [[CrossRef](#)]
11. Bhattacharya, S.; Phatake, R.S.; Nabha-Barnea, S.; Zerby, N.; Zhu, J.-J.; Shikler, R.; Lemcoff, N.G.; Jelinek, R. Fluorescent Self-Healing Carbon Dot/Polymer Gels. *ACS Nano* **2019**, *13*, 1433–1442. [[CrossRef](#)] [[PubMed](#)]
12. Tao, S.; Song, Y.; Zhu, S.; Shao, J.; Yang, B. A new type of polymer carbon dots with high quantum yield: From synthesis to investigation on fluorescence mechanism. *Polymer* **2017**, *116*, 472–478. [[CrossRef](#)]
13. Yu, S.; Kuan, C.; Feng, W.; Zhu, Y. Synthesis of Chitosan-Based Polymer Carbon Dots Fluorescent Materials and Application of Self-Assembled Drug-Loading. *Chin. Optic.* **2018**, *11*, 420–430.
14. Feng, H.; Pan, K.; Lv, X.; Yang, B.; Cui, Z. High performance polymer carbon dots for detection of chromium (VI) ions in water. *AIP Conf. Proc.* **2017**, *1829*, 20045. [[CrossRef](#)]
15. Yu, Y.; Tang, P.; Barnych, B.; Zhao, C.; Sun, G.; Ge, M. Design and Synthesis of Core-Shell Carbon Polymer Dots with Highly Stable Fluorescence in Polymeric Materials. *ACS Appl. Nano Mater.* **2019**, *2*, 6503–6512. [[CrossRef](#)]
16. Li, G.; Wang, F.; Liu, P.; Chen, Z.; Lei, P.; Xu, Z.; Li, Z.; Ding, Y.; Zhang, S.; Yang, M. Polymer dots grafted TiO₂ nanohybrids as high performance visible light photocatalysts. *Chemosphere* **2018**, *197*, 526–534. [[CrossRef](#)]
17. Robby, A.I.; Lee, G.; Lee, K.D.; Jang, Y.C.; Park, S.Y. GSH-responsive self-healable conductive hydrogel of highly sensitive strain-pressure sensor for cancer cell detection. *Nano Today* **2021**, *39*, 101178. [[CrossRef](#)]
18. Lu, S.; Sui, L.; Wu, M.; Zhu, S.; Yong, X.; Yang, B. Graphitic Nitrogen and High-Crystalline Triggered Strong Photoluminescence and Room-Temperature Ferromagnetism in Carbonized Polymer Dots. *Adv. Sci.* **2018**, *6*, 1801192. [[CrossRef](#)] [[PubMed](#)]
19. Xia, C.; Zhu, S.; Zhang, S.-T.; Zeng, Q.; Tao, S.; Tian, X.; Li, Y.; Yang, B. Carbonized Polymer Dots with Tunable Room-Temperature Phosphorescence Lifetime and Wavelength. *ACS Appl. Mater. Interfaces* **2020**, *12*, 38593–38601. [[CrossRef](#)]
20. Xia, C.; Tao, S.; Zhu, S.; Song, Y.; Feng, T.; Zeng, Q.; Liu, J.; Yang, B. Hydrothermal Addition Polymerization for Ultrahigh-Yield Carbonized Polymer Dots with Room Temperature Phosphorescence via Nanocomposite. *Chem. A Eur. J.* **2018**, *24*, 11303–11308. [[CrossRef](#)] [[PubMed](#)]
21. Vallan, L.; Urriolabeitia, E.P.; Ruipérez, F.; Matxain, J.M.; Canton-Vitoria, R.; Tagmatarchis, N.; Benito, A.M.; Maser, W.K. Supramolecular-Enhanced Charge Transfer within Entangled Polyamide Chains as the Origin of the Universal Blue Fluorescence of Polymer Carbon Dots. *J. Am. Chem. Soc.* **2018**, *140*, 12862–12869. [[CrossRef](#)] [[PubMed](#)]
22. Aji, M.P.; Wati, A.L.; Priyanto, A.; Karunawan, J.; Nuryadin, B.W.; Wibowo, E.; Marwoto, P. Sulhadi Polymer carbon dots from plastics waste upcycling. *Environ. Nanotechnol. Monit. Manag.* **2018**, *9*, 136–140. [[CrossRef](#)]
23. Jiang, Y.J.; Lin, M.; Yang, T.; Li, R.S.; Huang, C.Z.; Wang, J.; Li, Y.F. Nitrogen and phosphorus doped polymer carbon dots as a sensitive cellular mapping probe of nitrite. *J. Mater. Chem. B* **2019**, *7*, 2074–2080. [[CrossRef](#)] [[PubMed](#)]
24. Kang, E.B.; Sharker, S.M.; In, I.; Park, S.Y. Pluronic mimicking fluorescent carbon nanoparticles conjugated with doxorubicin via acid-cleavable linkage for tumor-targeted drug delivery and bioimaging. *J. Ind. Eng. Chem.* **2016**, *43*, 150–157. [[CrossRef](#)]
25. Zhu, S.; Wang, L.; Zhou, N.; Zhao, X.; Song, Y.; Maharjan, S.; Zhang, J.; Lu, L.; Wang, H.; Yang, B. The crosslink enhanced emission (CEE) in non-conjugated polymer dots: From the photoluminescence mechanism to the cellular uptake mechanism and internalization. *Chem. Commun.* **2014**, *50*, 13845–13848. [[CrossRef](#)]
26. Liu, J.; Li, D.; Zhang, K.; Yang, M.; Sun, H.; Yang, B. One-Step Hydrothermal Synthesis of Nitrogen-Doped Conjugated Carbonized Polymer Dots with 31% Efficient Red Emission for In Vivo Imaging. *Small* **2018**, *14*, e1703919. [[CrossRef](#)]
27. Liu, M.-X.; Chen, S.; Ding, N.; Yu, Y.-L.; Wang, J.-H. A carbon-based polymer dot sensor for breast cancer detection using peripheral blood immunocytes. *Chem. Commun.* **2020**, *56*, 3050–3053. [[CrossRef](#)] [[PubMed](#)]
28. Yang, M.; Liu, M.; Wu, Z.; He, Y.; Ge, Y.; Song, G.; Zhou, J. Fluorescence enhanced detection of water in organic solvents by one-pot synthesis of orange-red emissive polymer carbon dots based on 1, 8-naphthalenediol. *Micro Nano Lett.* **2020**, *15*, 469–473. [[CrossRef](#)]
29. Xia, J.; Chen, S.; Zou, G.-Y.; Yu, Y.-L.; Wang, J.-H. Synthesis of highly stable red-emissive carbon polymer dots by modulated polymerization: From the mechanism to application in intracellular pH imaging. *Nanoscale* **2018**, *10*, 22484–22492. [[CrossRef](#)] [[PubMed](#)]
30. Zhao, L.; Li, H.; Liu, H.; Liu, M.; Huang, N.; He, Z.; Li, Y.; Chen, Y.; Ding, L. Microwave-assisted facile synthesis of polymer dots as a fluorescent probe for detection of cobalt(II) and manganese(II). *Anal. Bioanal. Chem.* **2019**, *411*, 2373–2381. [[CrossRef](#)]
31. Yang, S.; Wang, L.; Zuo, L.; Zhao, C.; Li, H.; Ding, L. Non-conjugated polymer carbon dots for fluorometric determination of metronidazole. *Microchim. Acta* **2019**, *186*, 1–9. [[CrossRef](#)] [[PubMed](#)]
32. Mishra, M.K.; Kundu, S.; De, G. Stable fluorescent CdS: Cu QDs and their hybridization with carbon polymer dots for white light emission. *J. Mater. Chem. C* **2016**, *4*, 1665–1674. [[CrossRef](#)]

33. He, C.; Yan, H.; Li, X.; Wang, X. Ultrafast preparation of polymer carbon dots with solid-state fluorescence for white light-emitting diodes. *Mater. Res. Express* **2019**, *6*, 065609. [[CrossRef](#)]
34. Sajjad, F.; Yan, Y.-J.; Margetić, D.; Chen, Z.-L. Synthesis and in vitro PDT evaluation of red emission polymer dots (R-CPDs) and pyropheophorbide- α conjugates. *Sci. Rep.* **2021**, *11*, 1–13. [[CrossRef](#)]
35. Liu, J.; Geng, Y.; Li, D.; Yao, H.; Huo, Z.; Li, Y.; Zhang, K.; Zhu, S.; Wei, H.; Xu, W.; et al. Deep Red Emissive Carbonized Polymer Dots with Unprecedented Narrow Full Width at Half Maximum. *Adv. Mater.* **2020**, *32*, e1906641. [[CrossRef](#)]
36. Qiao, Z.; Huo, Q.; Chi, M.; Veith, G.M.; Binder, A.J.; Dai, S. A Ship-In-A-Bottle Approach to Synthesis of Polymer Dots@Silica or Polymer Dots@Carbon Core-Shell Nanospheres. *Adv. Mater.* **2012**, *24*, 6017–6021. [[CrossRef](#)]
37. Tang, Y.; Zhou, X.; Xu, K.; Dong, X. One-pot synthesis of fluorescent non-conjugated polymer dots for Fe³⁺ detection and temperature sensing. *Spectrochim. Acta Part A Mol. Biomol. Spectrosc.* **2020**, *240*, 118626. [[CrossRef](#)]
38. Xia, J.; Zhuang, Y.-T.; Yu, Y.-L.; Wang, J.-H. Highly fluorescent carbon polymer dots prepared at room temperature, and their application as a fluorescent probe for determination and intracellular imaging of ferric ion. *Microchim. Acta* **2017**, *184*, 1109–1116. [[CrossRef](#)]
39. Xia, J.; Yu, Y.-L.; Wang, J.-H. Fe³⁺-Catalyzed low-temperature preparation of multicolor carbon polymer dots with the capability of distinguishing D₂O from H₂O. *Chem. Commun.* **2019**, *55*, 12467–12470. [[CrossRef](#)]
40. Zare-Moghadam, M.; Shamsipur, M.; Molaabasi, F.; Hajipour-Verdom, B. Chromium speciation by isophthalic acid-doped polymer dots as sensitive and selective fluorescent probes. *Talanta* **2020**, *209*, 120521. [[CrossRef](#)]
41. Lu, S.; Sui, L.; Liu, J.; Zhu, S.; Chen, A.; Jin, M.; Yang, B. Near-Infrared Photoluminescent Polymer-Carbon Nanodots with Two-Photon Fluorescence. *Adv. Mater.* **2017**, *29*. [[CrossRef](#)]
42. Zhu, S.; Song, Y.; Zhao, X.; Shao, J.; Zhang, J.; Yang, B. The photoluminescence mechanism in carbon dots (graphene quantum dots, carbon nanodots, and polymer dots): Current state and future perspective. *Nano Res.* **2015**, *8*, 355–381. [[CrossRef](#)]
43. Adrita, S.H.; Tasnim, K.N.; Ryu, J.H.; Sharker, S.M. Nanotheranostic Carbon Dots as an Emerging Platform for Cancer Therapy. *J. Nanotheranostics* **2020**, *1*, 6. [[CrossRef](#)]
44. Mao, L.; Gao, M.; Xue, X.; Yao, L.; Wen, W.; Zhang, X.; Wang, S. Organic-inorganic nanoparticles molecularly imprinted photoelectro-chemical sensor for α -solanine based on p-type polymer dots and n-CdS heterojunction. *Anal. Chim. Acta* **2019**, *1059*, 94–102. [[CrossRef](#)]
45. Hu, J.; Liu, S. Engineering Responsive Polymer Building Blocks with Host–Guest Molecular Recognition for Functional Applications. *Acc. Chem. Res.* **2014**, *47*, 2084–2095. [[CrossRef](#)]
46. Kickelbick, G. Concepts for the incorporation of inorganic building blocks into organic polymers on a nanoscale. *Prog. Polym. Sci.* **2003**, *28*, 83–114. [[CrossRef](#)]
47. Sharker, S.M.; Kim, S.M.; In, I.; Lee, H.; Park, S.Y. Target delivery of β -cyclodextrin/paclitaxel complexed fluorescent carbon nanoparticles: Externally NIR light and internally pH sensitive-mediated release of paclitaxel with bio-imaging. *J. Mater. Chem. B* **2015**, *3*, 5833–5841. [[CrossRef](#)]
48. Cheng, X.; Huang, Y.; Li, D.; Yuan, C.; Li, Z.-L.; Sun, L.; Jiang, H.; Ma, J. A sensitive polymer dots fluorescent sensor for determination of α -L-fucosidase activity in human serum. *Sens. Actuat. B Chem.* **2019**, *288*, 38–43. [[CrossRef](#)]
49. Song, Y.; Chen, J.; Hu, D.; Liu, F.; Li, P.; Li, H.; Chen, S.; Tan, H.; Wang, L. Ratiometric fluorescent detection of biomarkers for biological warfare agents with carbon dots chelated europium-based nanoscale coordination polymers. *Sens. Actuat. B Chem.* **2015**, *221*, 586–592. [[CrossRef](#)]
50. Phuong, P.T.M.; Ryplida, B.; In, I.; Park, S.Y. High performance of electrochemical and fluorescent probe by interaction of cell and bacteria with pH-sensitive polymer dots coated surfaces. *Mater. Sci. Eng. C* **2019**, *101*, 159–168. [[CrossRef](#)]
51. Abdullah Issa, M.Z.; Abidin, Z. Sustainable Development of Enhanced Luminescence Polymer-Carbon Dots Composite Film for Rapid Cd²⁺ Removal from Wastewater. *Molecules* **2020**, *25*, 3541. [[CrossRef](#)] [[PubMed](#)]
52. Zhu, S.; Meng, Q.; Wang, L.; Zhang, J.; Song, Y.; Jin, H.; Zhang, K.; Sun, H.; Wang, H.; Yang, B. Highly photoluminescent carbon dots for multicolor patterning, sensors, and bioimaging. *Angew. Chem.* **2013**, *125*, 4045–4049. [[CrossRef](#)]
53. Sun, B.; Zhao, B.; Wang, D.; Wang, Y.; Tang, Q.; Zhu, S.; Yang, B.; Sun, H. Fluorescent non-conjugated polymer dots for targeted cell imaging. *Nanoscale* **2016**, *8*, 9837–9841. [[CrossRef](#)] [[PubMed](#)]
54. Prianka, T.R.; Subhan, N.; Reza, H.M.; Hosain, M.K.; Rahman, M.A.; Lee, H.; Sharker, S.M. Recent exploration of bio-mimetic nano-material for potential biomedical applications. *Mater. Sci. Eng. C* **2018**, *93*, 1104–1115. [[CrossRef](#)] [[PubMed](#)]
55. Tao, S.; Feng, T.; Zheng, C.; Zhu, S.; Yang, B. Carbonized polymer dots: A brand new perspective to recognize luminescent carbon-based nanomaterials. *J. Phys. Chem. Lett.* **2019**, *10*, 5182–5188. [[CrossRef](#)] [[PubMed](#)]
56. Pirsaeheb, M.; Mohammadi, S.; Salimi, A.; Payandeh, M. Functionalized fluorescent carbon nanostructures for targeted imaging of cancer cells: A review. *Microchim. Acta* **2019**, *186*, 231. [[CrossRef](#)]
57. Hakim, L.; Nahar, N.; Saha, M.; Islam, M.S.; Reza, H.M.; Sharker, S.M. Local drug delivery from surgical thread for area-specific anesthesia. *Biomed. Phys. Eng. Express* **2020**, *6*, 015028. [[CrossRef](#)] [[PubMed](#)]
58. Kim, S.H.; In, I.; Park, S.Y. pH-Responsive NIR-absorbing fluorescent polydopamine with hyaluronic acid for dual targeting and synergistic effects of photothermal and chemotherapy. *Biomacromolecules* **2017**, *18*, 1825–1835. [[CrossRef](#)]
59. Li, Q.; Ohulchanskyy, T.; Liu, R.; Koynov, K.; Wu, D.; Best, A.; Kumar, R.; Bonoiu, A.; Prasad, P.N. Photoluminescent Carbon Dots as Biocompatible Nanoprobes for Targeting Cancer Cells in Vitro. *J. Phys. Chem. C* **2010**, *114*, 12062–12068. [[CrossRef](#)]

60. Son, J.; Yi, G.; Yoo, J.; Park, C.; Koo, H.; Choi, H.S. Light-responsive nanomedicine for biophotonic imaging and targeted therapy. *Adv. Drug Deliv. Rev.* **2019**, *138*, 133–147. [[CrossRef](#)]
61. Ali, E.S.; Sharker, S.M.; Islam, M.T.; Khan, I.N.; Shaw, S.; Rahman, A.; Uddin, S.J.; Shill, M.C.; Rehman, S.; Das, N.; et al. Targeting cancer cells with nanotherapeutics and nanodiagnosics: Current status and future perspectives. *Semin. Cancer Biol.* **2021**, *69*, 52–68. [[CrossRef](#)]
62. Sharker, S.M. Hexagonal Boron Nitrides (White Graphene): A Promising Method for Cancer Drug Delivery. *Int. J. Nanomed.* **2019**, *14*, 9983–9993. [[CrossRef](#)]
63. Sharker, S.M.; Lee, J.E.; Kim, S.H.; Jeong, J.H.; In, I.; Lee, H.; Park, S.Y. pH triggered in vivo photothermal therapy and fluorescence nanoplatform of cancer based on responsive polymer-indocyanine green integrated reduced graphene oxide. *Biomaterials* **2015**, *61*, 229–238. [[CrossRef](#)]
64. Kim, S.H.; Sharker, S.M.; Lee, H.; In, I.; Lee, K.D.; Park, S.Y. Photothermal conversion upon near-infrared irradiation of fluorescent carbon nanoparticles formed from carbonized polydopamine. *RSC Adv.* **2016**, *6*, 61482–61491. [[CrossRef](#)]
65. Sharker, S.M.; Kang, E.B.; Shin, C.I.; Kim, S.H.; Lee, G.; Park, S.Y. Near-infrared-active and pH-responsive fluorescent polymer-integrated hybrid graphene oxide nanoparticles for the detection and treatment of cancer. *J. Appl. Poly. Sci.* **2016**, *133*. [[CrossRef](#)]
66. Jeong, C.J.; Sharker, S.M.; In, I.; Park, S.Y. Iron oxide@ PEDOT-based recyclable photothermal nanoparticles with poly (vinylpyrrolidone) sulfobetaines for rapid and effective antibacterial activity. *ACS Appl. Mater. Interfaces* **2015**, *7*, 9469–9478. [[CrossRef](#)]
67. Sharker, S.M.; Kim, S.M.; Lee, J.E.; Choi, K.H.; Shin, G.; Lee, S.; Lee, K.D.; Jeong, J.H.; Lee, H.; Park, S.Y. Functionalized biocompatible WO₃ nanoparticles for triggered and targeted in vitro and in vivo photothermal therapy. *J. Control Release* **2015**, *217*, 211–220. [[CrossRef](#)]
68. Kim, S.H.; Lee, J.E.; Sharker, S.M.; Jeong, J.H.; In, I.; Park, S.Y. In Vitro and In Vivo Tumor Targeted Photothermal Cancer Therapy Using Functionalized Graphene Nanoparticles. *Biomacromolecules* **2015**, *16*, 3519–3529. [[CrossRef](#)]
69. Kim, Y.K.; Kang, E.B.; Kim, S.H.; Sharker, S.M.; Kong, B.Y.; In, I.; Lee, K.-D.; Park, S.Y. Visible-Light-Driven Photocatalysts of Perfluorinated Silica-Based Fluorescent Carbon Dot/TiO₂ for Tunable Hydrophilic–Hydrophobic Surfaces. *ACS Appl. Mater. Interfaces* **2016**, *8*, 29827–29834. [[CrossRef](#)]
70. Ji, T.; Guo, B.; Liu, F.; Zeng, Q.; Yu, C.; Du, X.; Jin, G.; Feng, T.; Zhu, S.; Li, F.; et al. Cathode and Anode Interlayers Based on Polymer Carbon Dots via Work Function Regulation for Efficient Polymer Solar Cells. *Adv. Mater. Interfaces* **2018**, *5*. [[CrossRef](#)]